

Decision-Focused Model-based Reinforcement Learning for Reward Transfer

Abhishek Sharma
SEAS, Harvard University
Allston, MA, USA
abhisheksharma@g.harvard.edu

Omer Gottesman
Amazon
New York, NY, USA
omergott@gmail.com

Sonali Parbhoo
Imperial College London
London, UK
s.parbhoo@imperial.ac.uk

Finale Doshi-Velez
SEAS, Harvard University
Allston, MA, USA
finale@seas.harvard.edu

ABSTRACT

Decision-focused (DF) model-based reinforcement learning has recently been introduced as a powerful algorithm that can focus on learning the MDP dynamics that are most relevant for obtaining high returns. While this approach increases the agent’s performance by directly optimizing the reward, it does so by learning less accurate dynamics from a maximum likelihood perspective. We demonstrate that when the reward function is defined by preferences over multiple objectives, the DF model may be sensitive to changes in the objective preferences. In this work, we develop the robust decision-focused (RDF) algorithm, which leverages the non-identifiability of DF solutions to learn models that maximize expected returns while simultaneously learning models that transfer to changes in the preference over multiple objectives. We demonstrate the effectiveness of RDF on two synthetic domains and two healthcare simulators, showing that it significantly improves the robustness of DF model learning to changes in the reward function without compromising training-time return.

KEYWORDS

model-based reinforcement learning, decision-focused learning, simple models

1 INTRODUCTION

Model-based reinforcement learning (MBRL) approaches focus on learning a transition model of the environment, and using this model for planning policies. Using simple model classes can be necessary for interpretability and data efficiency reasons. It has been shown that since the model’s limited representational capacity precludes modeling *everything* about the dynamics, optimizing the model parameters with respect to the *eventual return* of the planned policy may perform better than just minimizing prediction error (see for instance [14]). This type of model learning is referred to as *decision-focused (DF) learning* [27, 34] of the model.

By construction, DF learning prioritizes learning parts of the MDP dynamics most relevant for obtaining high rewards during training. Though desirable, in many instances DF learning can be seen as “overfitting” a dynamics model to the reward function at train time, and can perform poorly if the rewards change at deployment time. Yet changing reward functions are abundant in many domains: in healthcare, clinicians can shift their preferences over time to trade off long- and short-term health-effects or balance

the aggressiveness of treatments or other measures of a patient’s well-being [20]. More generally, domain experts often have a sense of key objectives they want a reward function to encapsulate, but may want to support different trade-offs when the objectives are competing. Ideally, we want to learn a dynamics model that is robust to changes in the reward preferences at deployment *i.e. one that performs well across different reward preferences in both training and testing*.

In this paper, we show that by “overfitting” to a specific reward function at training, a DF model may be sensitive to changes in the reward function, resulting in non-robust solutions at test time. Overfitting occurs when there are multiple solutions for learning a dynamics model that, when used for planning, will produce a good policy only for the training-phase reward function. Prior work by Futoma et al. [13] used the model’s optimal value function to constrain the maximum likelihood objective. This resulted in an MBRL method that focuses on information that is important for decision-making for a given reward function. However, this form of regularization for choosing a DF transition model among many candidates still suffers from the same issue as the MLE-based approach to learning the transition model: it may focus on parts of the transition dynamics that are irrelevant to planning under a *different but known set of rewards*. When learning a transition model, we don’t need to model everything about the true dynamics—and with simple model classes, we cannot model everything. From the perspective of planning for different rewards, it is important that we focus on learning the aspects that allow this transfer.

To overcome these challenges, we introduce a Robust Decision-Focused (RDF) learning approach designed to learn models that perform well across different reward preferences in both training and testing, when the transition dynamics of the environment stay the same. Conceptually, we do this by optimizing a model with respect to a range of possible reward functions, parameterized by *reward preference* w , in contrast to works that apply DF model learning to a single reward function [23, 32]. A solution in the DF learning scenario would be sensitive to the preference w , and thus fail to generalize across different reward settings. In contrast, our RDF model enables us to obtain more robust solutions that transfer better across different test-time rewards. It does so by trading off training performance (evaluated on train-time reward preference) with average performance (evaluated on a range of

test-time reward preferences). We develop a novel algorithm that allows us to perform such optimization efficiently.

Our contributions are as follows: First, we show that the DF solutions are often non-identifiable, and may not be robust to the choice of reward at test time. Next, we introduce the RDF model which allows us to focus on *all reward preferences parameterized by* w . Unlike a DF model, the RDF model produces smoother solutions in w that transfer better over varying reward preferences at deployment time, whilst remaining performant on training reward. We provide theoretical bounds for RDF model’s action-value function and show they are tighter than DF model’s bounds at test-time rewards. On a suite of synthetic and healthcare domains, we show that our RDF model outperforms the DF and MLE models, while effectively balancing training and average performance.

2 PRELIMINARIES AND BACKGROUND

2.1 Notation

Markov Decision Process In RL, a Markov Decision Process (MDP) M is defined as $M = (\mathcal{S}, \mathcal{A}, R, T_*, \gamma)$. \mathcal{S} is a state space, \mathcal{A} is an action space, $R(s, a)$ is a reward function, $T_*(s'|s, a)$ is a transition distribution function, and $\gamma \in [0, 1)$ is a discount factor.

The goal of the agent is to learn a policy $A_t = \pi(S_t)$ that maximises the expected return $J_{T_*, R}(\pi) = \mathbb{E}_{A_t \sim \pi} \left[\sum_{t=0}^{\infty} \gamma^t R(S_t, A_t) \right]$ for transition function T_* and reward R . The policy quality can also be measured by the Bellman optimality error,

$$L_{T_*, R}(\pi) = \mathbb{E} \left[\left| Q_{T_*, R}^\pi(s, a) - BQ_{T_*, R}^\pi(s, a) \right| \right], \quad (1)$$

where $Q_{T_*, R}^\pi(s, a)$ is the action-value function of π :

$$Q_{T_*, R}^\pi(s, a) \triangleq \mathbb{E} \left[\sum_{t=0}^{\infty} \gamma^t R(S_t, A_t) \mid s_0 = s, a_0 = a \right] \quad (2)$$

and B is the Bellman optimality operator induced by the transition T_* and reward R on action-value function Q :

$$BQ(s, a) \triangleq R(s, a) + \gamma \mathbb{E}_{T_*(s'|s, a)} \left[\max_{a'} Q(s', a') \right] \quad (3)$$

The optimal action-value function $Q_{T_*, R}^*$ is a fixed point of B , and can be obtained by minimizing the Bellman error in Eqn 1.

Reward Preferences We assume a reward function that linearly interpolates between K basis reward functions R_1 to R_k according to,

$$R_w(s, a) = \sum_{k=1}^K w_k R_k(s, a); \quad \sum_k w_k = 1 \quad (4)$$

where w_k denotes a preference for a particular basis, and the R_k ’s are assumed as given. In practice, these reward bases are competing reward functions that the practitioner considers important. For example, in cancer treatment, they would promote the treatment’s efficacy (R_1) and penalize the patient’s side-effects (R_2).

Model-based RL Model-based RL (MBRL) algorithms learn a transition model T_θ of the environment and use this model to plan a policy. Here, θ are the parameters of the model which need to be estimated. MBRL methods allow improved sample-efficiency and

generalizability [6]. Traditional methods [28, 33] use maximum-likelihood estimation to estimate θ (MLE-MBRL), which is equivalent to minimizing the KL divergence between the transition model and the true dynamics:

$$\theta_{\text{MLE}} \leftarrow \arg \min_{\theta} \mathbb{KL}(T_* || T_\theta) \quad (5)$$

Since the MLE objective does not directly optimize for the objective of discounted returns, it can fail to find optimal policies when the model capacity is limited [11, 19, 23]. For example, an MLE model may “waste” its capacity on modeling an action that the optimal policy will never take, at the expense of differentiating between two near-optimal actions because it does not take into account the policies learned with the model.

Decision-focused Model-based RL (DF-MBRL). DF-MBRL considers the full computational graph of how the transition model T_θ affects the performance of the policy $\pi^*(\theta, R)$:

$$\theta \rightarrow T_\theta \rightarrow Q_{T_\theta, R}^* \rightarrow \pi^*(\theta, R) \rightarrow L_{T_*, R}(\pi^*(\theta, R)) \quad (6)$$

where $L_{T_*, R}$ is the Bellman optimality error, but we can also use the expected return $J_{T_*, R}$. The policy $\pi^*(\theta, R)$ is the optimal policy for the transition model T_θ and reward function R , and is computed by minimizing $L_{T_\theta, R}(\pi)$. $L_{T_*, R}(\pi^*(\theta, R))$ depends on θ through the policy $\pi^*(\theta, R)$, and on $\pi^*(\theta, R)$ directly. We use the notation $L_{T_*, R}(\theta)$ or $L_{T_*, R}(\pi^*)$ to show dependence on θ or π^* respectively. DF-MBRL directly optimizes for the performance of the policy on the true transition T_* :

$$\theta_{\text{DF}} \leftarrow \arg \min_{\theta} L_{T_*, R}(\theta) \quad (7)$$

In settings where the model class of T_θ cannot represent T_* , the decision-focused model can outperform the maximum-likelihood model [12, 19]. However, there can be several model parameters θ whose policy has high performance on the true environment [14, 23], i.e. the DF model is non-identifiable.

The main limitation of DF-MBRL is that the model is optimized for *one specific reward function*, R . While this is not an issue in settings where the reward function is not expected to change, this can be problematic in settings where the reward function is expected to change—or simply not known precisely at training time.

3 RELATED WORK

Our work is closely related to methods in decision-focused model-based RL, multi-objective RL, and reward-transfer RL literatures.

Decision-Focused Model-based Reinforcement Learning Several works have developed algorithms for decision-focused (DF) model-based reinforcement learning [12, 13, 19, 23, 32]. These works focus on building simple models, where the transition model cannot represent the true transition dynamics, that can be used for planning. In contrast to these, we consider the setting where the learned model must be re-used for different reward functions.

Grimm et al. [14] and Nikishin et al. [23] note that DF models can be non-identifiable for a given reward function. Both suggest this can be a good thing: if the only evaluation metric is the return of the RL agent (i.e. the DF objective), it is easier to find an optimal solution when multiple equivalent solutions of the DF objective exist. However, they do not consider the robustness of different DF solutions to changes in reward function. In contrast, we show that

the DF objective does not optimize for robustness, and may find a solution that is not robust to changes in reward. Furthermore, we exploit this non-identifiability of models with respect to the performance of the agent to find a solution that generalizes better to the changed reward function.

RL with changing objectives Multi-Objective RL (MORL) and reward-robust RL aim to train agents to perform well on multiple reward functions [1, 5, 7, 17, 20, 22]. The most common setting addressed in the MORL literature involves rewards functions linearly combined using a weight called *preference* [1, 5, 16, 20, 22, 35]. We make the same assumption. In both MORL and robust RL, the transition dynamics model (and potentially uncertainty about it) is either explicitly or implicitly (via data) provided as input to the algorithm. The algorithm’s goal is to then output a policy that is robust, or can be efficiently recomputed if preferences change. In contrast, our aim here is to *learn a transition model* which will produce robust policies when optimized for different reward functions.

There are a few exceptions—[31, 33, 35] propose MORL algorithms which learn a transition model, but do so (a) by only using $\{(S_t, A_t, S_{t+1})\}$ transitions to learn the model, and (b) by making strong assumptions on the state space (e.g. discrete) or the model dynamics (e.g. SIR model in epidemiology). Importantly, their model is learned *before* it is used for the MORL step (i.e. model learning does not take into account the policy from the MORL step). In contrast, our model is learned *along with* the MORL step: we consider which transition model will result in a good policy during the MORL step.

Transfer Learning across Rewards Under Fixed Dynamics The setting of fixed MDP transition dynamics but different reward functions has also been addressed in the transfer learning literature. The key difference between the transfer learning literature and the multi-objective learning literature in which our work is centered is that our method is not designed to adapt to a new task with new data, but rather find one model which applies well to multiple tasks at once. Barreto et al. [4] performs transfer learning in situations where only the reward function differs, by using successor features to decouple a policy’s dynamics from expected rewards. Reinke and Alameda-Pineda [24] relax some of the assumptions that rewards may be decomposed linearly into successor features for knowledge transfer. Unlike both of these, our work makes no assumptions about the form of the reward function. The idea of using successor features to express the reward function is complementary and can also be incorporated into our approach.

4 PROBLEM SETTING

Our problem setting consists of two distinct phases: the learning phase and deployment phase.

Learning phase. In the *learning phase*, we are given access to the true transition function T_* (in the form of a simulator) and the reward function $R_{\bar{w}}$, where \bar{w} is the learning-phase reward preference. We are also provided a *deployment-phase* reward preference distribution. During the learning phase, we can simulate trajectories from the simulator without any restrictions. At the end of this phase, we must build a model of the simulator that is simple enough, but also allows us to plan high-performing policies for different reward preferences.

Deployment phase. During the *deployment phase*, we are no longer given access to the true transition function. In addition to the learning-phase reward function $R_{\bar{w}}$, we are given a deployment-phase reward function R_w that our model should transfer to. Note that while the deployment-phase reward preference w is unknown during the learning phase, we know the distribution $P(w)$ from which w comes from. In addition to doing well on $R_{\bar{w}}$, we should be able to re-plan high-quality policies on the deployment-phase reward functions. Such a setting is common in healthcare applications, where learning-phase and deployment-phase rewards may correspond to needs of different patient populations [20]. For example, in cancer treatment, different patients are more susceptible to developing adverse side effects from the treatment and would therefore need lower dosages. \bar{w} would encode the preferences for a known patient population, and $P(w)$ would correspond to the set of preferences the doctor wants to support.

Why simple models? In healthcare applications, the true environment dynamics are very complex and expensive to access. For example, organs-on-chips models of a lung alveolus can faithfully simulate lung cancer dynamics but are expensive [15, 18]. For this reason, simple models are learned to understand disease dynamics and to simulate data for reasoning and policy learning. While complex computational models can be used to simulate highly accurate data, they can be expensive to run and their access can be siloed. Simple models are desirable for reduced computational complexity, improved interpretability [8], and to *only* capture the dynamics relevant for the problem.

Choosing $P(w)$. Although knowledge of $P(w)$ might seem to be a strong assumption, in real-world settings it is often possible to define a $P(w)$ using reasonable boundary conditions. For example, in many healthcare applications, patients can express their preferred trade-off between the aggressiveness of the treatment and its side-effects. A domain expert will both know what kinds of trade-offs are common in their domain, as well as what is the common span of preferences along these trade-offs. Access to this type of knowledge motivates our use of a uniform distribution over a given range of w , encoding the idea that domain experts can often easily provide reasonable ranges of preferences, but not probabilities over the preferences. Our goal then becomes to be robust over the entire range of reasonable preferences.

5 PROPOSED FRAMEWORK: ROBUST DECISION-FOCUSED MODEL-BASED RL

Our goal is to learn a *simple, decision-focused* transition model that produces high-performing policies for the rewards encountered during *both* the learning and deployment phases.

While DF-MBRL can learn a model that performs well on the true environment, it is tied to a specific reward function that was used during training. To alleviate this drawback of DF-MBRL, we leverage the non-identifiability of DF solutions—among the many DF solutions on the learning-phase reward function, we choose the one that would perform well on multiple possible deployment-phase reward functions.

We formalize this notion in the following Robust Decision-Focused (RDF) MBRL objective:

$$\begin{aligned} \theta_{\text{RDF}} \leftarrow \arg \min_{\theta} \mathbb{E}_{P(\bar{w})} [L_{T_s, R_w}(\theta)] \\ \text{s.t. } J_{T_s, R_w}(\pi^*(\theta, R_{\bar{w}})) \geq \delta \end{aligned} \quad (8)$$

which optimizes the model parameters θ to have high performance on the (yet unknown) deployment reward function R_w , while simultaneously achieving high performance on the learning-phase reward function $R_{\bar{w}}$. Below we first provide a theoretical analysis of this objective and then describe our optimization approach.

5.1 Theoretical Analysis

We theoretically characterize the quality of policies achieved by RDF algorithm, and show that our RDF objective can achieve better policies than DF-MBRL in the deployment phase. Hence, given the same representational capacity, RDF will learn a model that better approximates the optimal Q function across the range of possible deployment rewards. We provide the proof in the supplement.

THEOREM 5.1. *Let $R_{\bar{w}}$ be the learning-phase reward function with preference \bar{w} , and R_w be the reward function with an arbitrary preference w . Let Q_w^* be the optimal action-value function for the true MDP for reward function R_w . Let $B_w, \hat{B}_w^{\text{DF}}, \hat{B}_w^{\text{RDF}}$ denote the Bellman optimality operators under the true dynamics, DF model, and RDF model respectively.*

Assume \hat{Q}_w^{DF} and \hat{Q}_w^{RDF} are fixed points under \hat{B}_w^{DF} and \hat{B}_w^{RDF} respectively. Further assume that the reward function is bounded, $R_w(s, a) \in [0, r_{\max}] \forall s, a, w$.

DF Case. *Consider a DF model trained on $R_{\bar{w}}$. If the Bellman operator induced by the DF model achieves the error $\sup_{s,a} |B_w \hat{Q}_w^{\text{DF}}(s, a) - \hat{B}_w^{\text{DF}} \hat{Q}_w^{\text{DF}}(s, a)| = \epsilon_w^{\text{DF}}$, then*

$$Q_w^*(s, a) - \hat{Q}_w^{\text{DF}}(s, a) \leq \frac{\epsilon_w^{\text{DF}}}{(1-\gamma)} \quad \text{for } w = \bar{w} \quad (9)$$

$$Q_w^*(s, a) - \hat{Q}_w^{\text{DF}}(s, a) \leq \gamma \frac{r_{\max}}{(1-\gamma)^2} \quad \forall w \neq \bar{w} \quad (10)$$

RDF Case. *Consider the RDF model trained with learning-phase preference \bar{w} and deployment-phase reward preference distribution $P(w)$. For a $w \in P(w)$, if the Bellman operator \hat{B}_w^{RDF} induced by the RDF model achieves the error $\sup_{s,a} |B_w \hat{Q}_w^{\text{RDF}}(s, a) - \hat{B}_w^{\text{RDF}} \hat{Q}_w^{\text{RDF}}(s, a)| = \epsilon_w^{\text{RDF}}$, then*

$$Q_w^*(s, a) - \hat{Q}_w^{\text{RDF}}(s, a) \leq \frac{\epsilon_w^{\text{RDF}}}{(1-\gamma)} \quad (11)$$

For, $w \neq \bar{w}$, the RDF bound is tighter since we explicitly optimize ϵ_w^{RDF} whereas $\gamma \frac{r_{\max}}{(1-\gamma)^2}$ is constant.

Empirical validation of Theorem. We empirically validate our theorem in Figure 1 using a simulated MDP with twenty states and two actions. (we describe the MDP and provide the simulation code in the supplement). We plot the suboptimality gaps $\max_{(s,a)} |Q_w^*(s, a) - \hat{Q}_w^{\text{DF}}(s, a)|$ and $\max_{(s,a)} |Q_w^*(s, a) - \hat{Q}_w^{\text{RDF}}(s, a)|$ for learning-phase (\bar{w}) and deployment-phase (w) preferences. We observe that the RDF bound (red dashed line) is tighter than the DF bound (blue dashed line) for $w \neq \bar{w}$. *More importantly*, there exist w values for which the RDF bound is tighter than the observed DF suboptimality gap (blue solid line is above the red dashed line

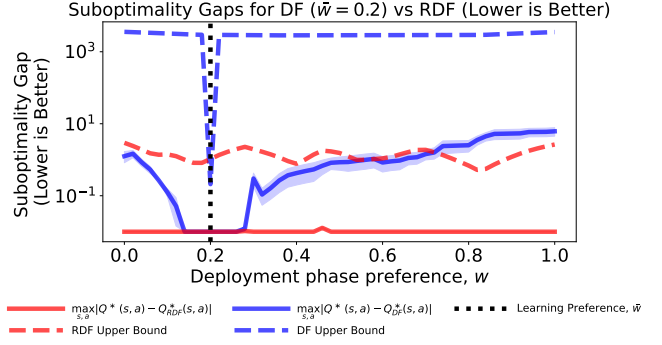


Figure 1: Theoretical bounds on the suboptimality gap of RDF models (red dashed line) confirm that RDF models can achieve a better (i.e. lower) suboptimality gap than DF models (blue solid line) away from the learning-phase reward preference \bar{w} . In this example, the RDF bound guarantees better-than-DF performance for $w > 0.8$. Learning-phase preference \bar{w} is 0.2 and $P(w)$ is uniform on $[0, 1]$.

in Figure 1). For these w values, our bound guarantees that RDF model's suboptimality gap will be lower than the DF model's gap. This is possible because the RDF objective included these w values.

5.2 Optimizing of RDF objective

Since optimizing the constrained form of RDF objective in Eqn 8 can be challenging, we rewrite it using a Lagrange multiplier $\lambda > 0$:

$$L_{T_s}^{\text{RDF}}(\theta, \lambda) = \mathbb{E}_{P(w)} [L_{T_s, R_w}(\theta)] + \lambda L_{T_s, R_{\bar{w}}}(\theta) \quad (12)$$

The limit $\lambda \rightarrow \infty$ recovers the DF objective, while setting $\lambda = 0$ ignores performance on the learning-phase reward and focuses on overall robustness with respect to deployment-phase reward distribution, $P(w)$.

Evaluating the objective. As discussed in Sec 4, a uniform distribution is a reasonable assumption for $P(w)$ in real-world settings. We approximate the expectation in Eqn 12 using the trapezoid method. Specifically, we construct \mathcal{W} , a set of uniformly-spaced w values in the support of P and use it to approximate the expectation:

$$\mathbb{E}_{w \sim P(w)} [L_{T_s, R_w}(\theta)] \approx \frac{1}{|\mathcal{W}|} \sum_{w \in \mathcal{W}} L_{T_s, R_w}(\theta) \quad (13)$$

When w high dimensional, we can use a more appropriate sampling method, and if $P(w)$ is not uniform, we can use importance weights to approximate the expectation more accurately. The choice of the sampling method is orthogonal to the RDF objective, and we proceed with a uniform grid for simplicity.

Computing the gradient. We employ implicit differentiation to compute gradients through the policy learning step [23, 32], and use the chain rule to compute the gradient of the RDF objective:

$$\frac{\partial L_{T_s, R}(\theta)}{\partial \theta} = \underbrace{-\frac{\partial L_{T_s, R}(\pi^*)}{\partial \pi}}_{\text{Grad Bellman}} \cdot \underbrace{\left[\frac{\partial^2 L_{T_s, R}(\pi^*)}{\partial \pi^2} \right]^{-1} \frac{\partial^2 L_{T_s, R}(\pi^*)}{\partial \pi \partial \theta}}_{\text{Implicit Grad of } \pi^* \text{ w.r.t } \theta} \quad (14)$$

Algorithm 1 General Robust Decision-Focused RL Algorithm

input Initial model parameters θ , learning reward preference \bar{w} , deployment reward preferences $\mathcal{W}, P(w)$, reward basis functions R_1, \dots, R_k
Initialize Q-function parameters $\phi_{\bar{w}}, \{\phi_w : w \in \mathcal{W}\}$
repeat
 for $w \in \{\bar{w}\} \cup \mathcal{W}$ **do**
 Using model T_θ and reward function R_w , update action-value function $Q_{T_\theta, R_w}^*(\phi_w)$.
 Compute policy $\pi^*(\theta, R_w)$ using the action-value function.
 Compute Bellman error $L_{T_\theta, R_w}(\pi^*(\theta, R_w))$.
 end for
 Update θ using the Bellman errors as per Eqn 14.
until the Bellman error converges.

Choosing a policy planner. Depending on the model parameterization, we can use an appropriate planning algorithm to learn the policy. The choice of the algorithm is orthogonal to the RDF objective, with the only requirement being that the algorithm can compute the gradient of the policy with respect to the model parameters. However, choosing a specific simple model class enables fast planning, e.g. Value Iteration (VI) for discrete states and Linear Quadratic Regulator (LQR) for continuous states with linear dynamics. For example, in the cancer simulator we describe in Sec 7.1, an LQR planner returned an optimal policy in less than a second because we used a linear transition model, while a Deep Q Network (DQN) [21] took approximately one hour to train.

Another consideration is that we need a Q-function for each w in the grid \mathcal{W} (Eq 13), especially in the case where Q-function is a neural network. When using a DQN to represent the Q-function, we used the same network to compute the Q-values for each w , which allowed us to amortize the cost of learning the Q-function across different w 's. We further discuss the implementation details in the supplement. Algorithm 1 presents the general RDF algorithm.

6 SYNTHETIC ENVIRONMENTS

We demonstrate the use of the RDF algorithm on a wide variety of simple model classes, including tabular representation, linear dynamics, and sparse neural networks. We first evaluate our RDF algorithm on two synthetic environments, where we can control the complexity of the environment and the reward preferences. We later evaluate our algorithm on two complex healthcare simulators, one for cancer treatment and one for HIV treatment. In each of these environments, we can simulate from the true simulators only during the learning phase and must learn a *simple* model that can be used to plan policies during the deployment phase.

Baselines. We compare the performance of our RDF approach to methods that are relevant to our setting, i.e., (a) the algorithm must output a simple model of transition dynamics, and (b) the learned model must transfer to multiple reward preferences. As identified in the Related Works (Sec 3), existing methods satisfy one of these requirements, but not both. We do not compare with model-based MORL methods [31, 33, 35] since they do not fit our setting for two reasons: (a) they only perform a single planning step and only *evaluate* the planned policy on different preferences, and

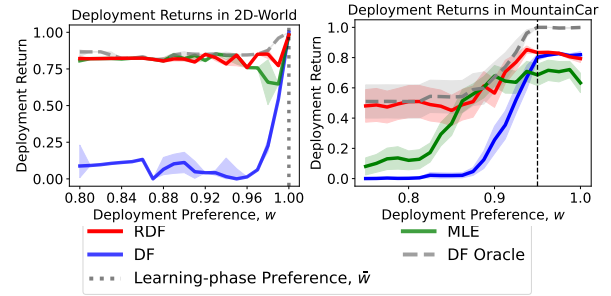


Figure 2: RDF outperforms DF and MLE models by achieving high returns across the deployment preferences on both 2D-World and MountainCar.

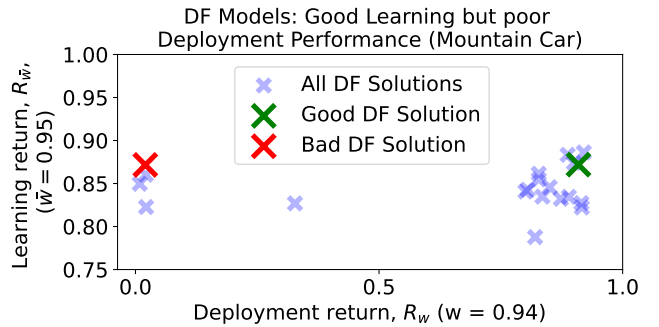


Figure 3: DF models can return solutions that transfer poorly to deployment preferences: some DF solutions transfer well (green) while others transfer poorly (red) to other preferences.

(b) they do not consider the learning of restricted models informed by the MORL step (they just do MLE/Bayesian model learning). To consider the best one can do with the constraint of a restricted model class, we train a DF-Oracle model that has access to the true transition dynamics during the deployment phase. Therefore, we compare RDF against DF and MLE (trained once on the training phase setting), as well as DF-Oracle (trained for each deployment phase setting).

Metrics. We evaluate the performance of RDF, DF, MLE, and DF-Oracle on the average deployment-phase return, denoted as J_{avg} , and the learning-phase return, denoted as $J_{\bar{w}}$. We scale all returns to $[0, 1]$ by using the maximum and minimum observed returns for a given reward preference. This ensures that different weight preferences (with different return ranges) are comparable to each other, and J_{avg} is not dominated by a single w value. We report the means and standard errors across 10 random seeds.

6.1 2D-World Environment

We construct a navigational task with two-dimensional continuous states $\in R_+^2$ and two-dimensional actions in $\{[0, 1]^T, [1, 0]^T\}$. The agent starts at state $[0, 0]^T$ and the episode ends if any of the states crosses value 25. The transition model is given by $s' \leftarrow s + \theta \odot \mathbf{a}$, where the true model's parameters are $\theta = \theta^* = [1.5, 5]^T$. For a physical interpretation, the θ parameters can be thought of as

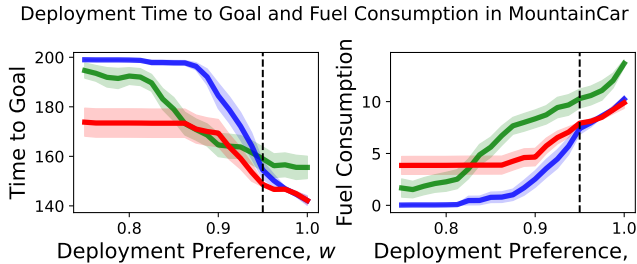


Figure 4: RDF model satisfies the requirements of reaching the goal early and saving fuel than DF and MLE models. DF models save fuel but also fail to reach the goal.

slippage coefficients for the two state dimensions. If θ is higher, the agent will slip more for an action it takes in that dimension.

Reward function. The first reward basis function R_1 only depends on the first state dimension S_1 . The second reward basis function R_2 is only a function of S_2 .

$$R_1(S) = \begin{cases} 5, & \text{if } S_1 \leq 2.5 \\ -1, & \text{o/w.} \end{cases}; \quad R_2(S) = \begin{cases} \frac{20}{17}S_2^2 - 1, & \text{if } S_2 \leq 13 \\ -201, & \text{o/w.} \end{cases}$$

The first reward function incentivizes the agent to stay in the region $S_1 \leq 2.5$, so knowing the correct value of S_1 is important to learn a good policy. The second reward’s value increases with S_2 until $S_2 = 13$ (a cliff), after which the agent reaches a region of large negative rewards. Without knowing the correct value of S_2 it will end up in, the agent would find it hard to learn a good policy.

Transition model learning. We restrict the model class to $\theta = \theta_c [1, 1]^T$, where θ_c is a scalar parameter, which corresponds to a subspace of the full parameter space not containing the true model parameters θ^* . The environment is challenging because the model forces the agent to either be too aggressive or too conservative in at least one of the state dimensions. For example, if it believes the slippage in the second dimension is smaller than it actually is (i.e. $\theta_c < \theta_2^*$), it will take aggressive steps in the second dimension and will fall off the cliff at $S_2 = 13$.

Since the learning-phase reward only depends on the first state dimension S_1 , the DF model θ_{DF} learns a value close to θ_1^* and can ignore the second state dimension S_2 without losing performance on the learning-phase reward function. The RDF model θ_{RDF} should reasonably estimate slippage in both the first and second state dimensions to achieve high performance. The MLE model θ_{MLE} learns the value $(\theta_1^* + \theta_2^*)/2$ for a uniform random policy.

We set the learning-phase reward preference to $\bar{w} = 1$ (i.e. $R_w = R_1$), and the deployment-phase reward preferences range to $w \in [0.8, 1]$. We create a grid of 50 θ values in the range $[0, 6]$ and compute the optimal policy’s return for θ . We use Fitted Q-Iteration [9] to learn a deterministic policy for any θ .

6.2 Mountain Car Environment

We compare the methods on the multi-objective mountain car problem [30]. In this environment, an underpowered car is positioned in a valley between two mountains on a one-dimensional track. The agent must build momentum by moving between the two mountains until the car has sufficient momentum to reach its goal. The

states are in \mathbf{R}^2 and correspond to the current position and velocity. The actions are in $\{-1, 0, 1\}$ and correspond to accelerating backward, not accelerating, and accelerating forwards respectively. An episode runs for a maximum of 200 steps.

Reward function. The first reward basis function R_1 is a penalty of -1 for each time step, whereas R_2 is a penalty of -0.1 each time the car accelerates as a proxy for fuel consumption. In the single-objective problem focusing solely on R_1 , the agent only needs to reach the goal in the fewest number of steps. With R_2 , we force the agent to exhibit prudence in its use of acceleration.

Transition model learning. While the true dynamics follow the equations of motion, we learn a tabular representation of the transition dynamics by discretizing the state space, which is frequently used in RL [29]. We split the position and velocity to 15 bins each, resulting in a total of 225 states. We can then use Value Iteration (VI) to derive the optimal policy at each step of the optimization. We set the learning preference to $\bar{w} = 0.95$, and the deployment preferences range to $w \in [0.75, 1]$. The discount factor is 1.

Conclusions from synthetic domains

DF models can be non-identifiable. Fig 3 shows that multiple DF solutions can have very different performance on deployment-time preferences in the MountainCar environment. For $w = 0.94$, the performance is high for one DF solution (green marker) whereas it is very poor (red marker) for another solution. This provides evidence that transfer in DF can be problematic without additional specifications, which RDF provides in form of average performance.

RDF models are more robust to reward function changes. Left panels of Fig 2 demonstrate the robustness of the RDF models when subjected to reward preferences away from their training settings. Unlike the DF and MLE solutions, RDF achieves near-optimal performance for the model class in both domains, with almost no degradation in learning-phase return. Performance of the DF model degrades significantly away from the learning-phase reward preference that it was trained on. MLE tends to transfer better than DF in both cases—but not as well as our RDF approach.

RDF offers significant advantages in optimizing trade-offs between objectives. The RDF agents consistently reached the goal faster than DF and MLE agents, even as fuel costs increased, all while maintaining reduced acceleration levels. This suggests that RDF transition models capture the effect of all actions much better than DF and MLE models. When transferring to a preference characterized by higher fuel costs, the DF models failed to even reach the goal.

7 HEALTHCARE SIMULATORS

Now we apply our RDF approach to two more complex environments relevant to our intended application: healthcare simulators.

7.1 Healthcare Simulator: Cancer Treatment

The focus of this cancer simulator is on optimizing dosing strategies to reduce mean tumor diameters (MTDs) for patients undergoing chemotherapy for the drug temozolomide (TMZ) [36]. The domain utilizes a tumor growth inhibition (TGI) model that captures the growth kinetics of diffuse low-grade gliomas (LGG) during and after chemo- and radiotherapy (CRT) of patients [25]. The 5-dimensional

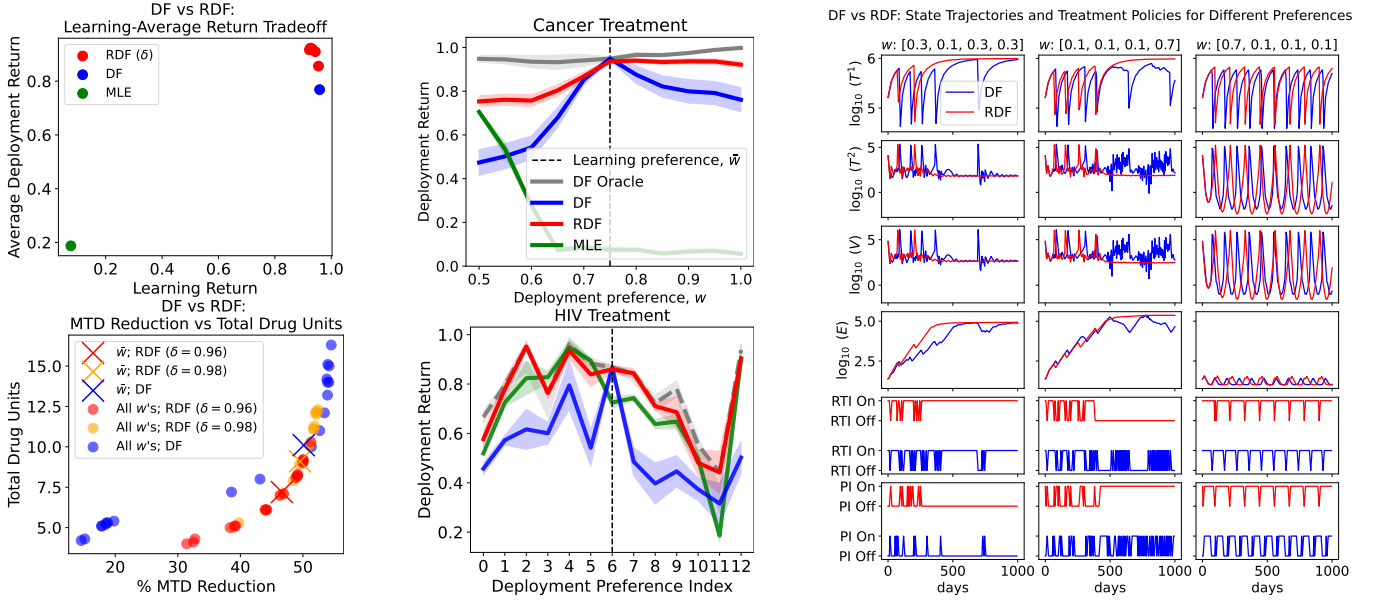


Figure 5: Results for Healthcare Simulators: Left: The learning-vs-average return plot shows how RDF models balance learning and average performance: RDF loses much less in learning return, than it gains in average return. The trade-off between Cancer environment’s objectives illustrates how RDF models (red and orange) achieve reductions in tumor diameter, even in low-drug-dose scenarios (they are further right of DF models (blue)). A model achieving a perfect trade-off would be in the bottom-right corner of the plot. Middle: RDF achieves superior average-case performance and covers DF’s performance across preferences for both domains. Right: RDF and DF models on three different reward preferences (columns) in the HIV domain. In the left column, RDF better adheres to the higher penalty for the Protease Inhibitor (PI) drug by giving fewer doses but still achieves comparable viral load reduction (V). In the middle column, RDF is again better at keeping the cytotoxic T-cells count (E) high, as required by a higher weight for E . Both models manage to keep the V low in the right column.

states $S_t = (M_t^1, M_t^2, M_t^3, C_t, t)$, consisting of the patient’s mean tumor diameters, drug concentration, and current time-step to ensure the Markovian assumption is met. The actions are discrete, in $\{0, 1\}$, and correspond to whether the drug is administered or not.

Reward function The paper introducing this simulator [36] included a reward function that can be interpreted as having two components: one that promotes a reduction in overall tumor size, and another that penalizes side-effects from using high concentrations of drugs. That is,

$$R_1(M_t, A_t, M_{t+1}) = \begin{cases} c_1(M_t - M_{t+1}) + (M_0 - M_T), & \text{if } t = T - 1. \\ c_1(M_t - M_{t+1}), & \text{otherwise.} \end{cases} \quad (15)$$

$$R_1(S_t, A_t, S_{t+1}) = -c_2 C_{t+1}$$

where $M_t = M_t^1 + M_t^2 + M_t^3$ is the total mean tumor diameter at time t . The parameters c_1 and c_2 are constants set to .1 and .5 in the original paper, after observing that these values led to sufficient MTD reduction in the patient population. Notably, these parameters do not take into account the range of preferences that a clinician may want to balance in terms of MTD reduction and side-effects. This is an important consideration in the real-world settings [20].

Transition model learning The environment dynamics follow TGI model, which is a system of ordinary differential equations (ODEs) that describe the evolution of the tumor size over time. We learn a linear model class to map (S_t, A_t) to S_{t+1} and use the learned model

to plan policies for different reward preferences. The linear model class and linear reward function allow us to use a Linear Quadratic Regulator (LQR) to plan policies.

We set the learning-phase preference \bar{w} to be 0.75, and the deployment phase preference range to $w \in [0.5, 1]$. We employed a Linear Quadratic Regulator (LQR), which leverages the advantages of the linear model class and linear reward function to efficiently plan policies. We set constraint values δ in the RDF objective (Eq 1) to $\delta \in \{0.95, 0.98, 1\}$ times the DF return. We did not try lower δ values because the unconstrained RDF model gives a high enough learning-phase return of 0.95 times the DF return.

Conclusions from Cancer Simulator

RDF models consistently learn a higher-return policy when evaluated on deployment-phase rewards compared to DF and MLE (Fig 5, upper middle). Note that the constraint on the learning return (δ) enables RDF to trade-off learning-phase and average return (Fig 5, upper left). Typically, the lower the constraint δ , the higher the average-case performance we can achieve. However, even for the same learning-phase return as DF, RDF model achieves a higher average return.

RDF offers significant advantages in optimizing trade-offs between clinical objectives (Fig 5, lower left) These trade-offs can be particularly relevant when considering individual patient preferences

and tolerances. For patients with low tolerance to side-effects (i.e. treatment constrained to 4-6 doses), RDF demonstrates MTD reduction of approximately 35%, well above the 20% reduction by DF. Even for patients with high tolerance to side-effects, RDF remains competitive, achieving an MTD reduction similar to DF, at 50%. These findings underscore the versatility and effectiveness of RDF in optimizing dosing regimens based on patient-specific needs and preferences. We provide detailed trajectories generated by both RDF and DF models in the supplement.

7.2 Complex Healthcare Simulator: HIV Treatment

In this domain, we want to determine an effective treatment strategy for patients with HIV. A patient’s 6-dimensional state $S_t = (T_t^1, T_t^2, T_t^{1*}, T_t^{2*}, V_t, E_t)$ is characterised by the number of infected and uninfected CD4+ T-cells (T^1) and macrophages (T^2), viral load (V) and cytotoxic T-cells (E) at each time point respectively. The protocol allows for drugs to be administered every five days based on a patient’s state by choosing one of four possible discrete actions A_t of whether or not to use a Reverse Transcriptase Inhibitor (RTI) or Protease Inhibitor (PI). The goal is to bring a patient’s viral load below detection limits i.e. below 40 copies/ml.

Reward function. So far, our examples have involved trade-offs between two reward bases. The HIV environment has more trade-offs: the reward function weighs four basis functions [10]:

$$R_1(S_t, A_t) = -\log_{10} V_t \quad R_2(S_t, A_t) = -c_1 A_t [0] \quad (16)$$

$$R_3(S_t, A_t) = -c_2 A_t [1] \quad R_4(S_t, A_t) = \log_{10} E_t, \quad (17)$$

where $c_1 = 2 \log_{10}(0.7)$ and $c_2 = 2 \log_{10}(0.3)$. R_1 prioritizes minimizing the blood viral load and R_4 prioritizes maximizing the immune response. R_2 and R_3 penalize the RTI and PI actions.

Transition model learning. The environment dynamics follow a set of ODEs describing the evolution in a patient’s viral load, macrophages, infected and uninfected T-cells and cytotoxic T-cells (see Adams et al. [2] for details). We use a neural network (NN) of 1 layer with 32 hidden nodes with L1 norm 5. Our inputs to the network correspond to the six state variables and 4 one-hot encoded actions.

Training details. We set the $\bar{w} = [0.25, 0.25, 0.25, 0.25]$. The deployment preference weights range (w) was set to the simplex formed by spanning points $\{[w_1, w_2, w_3, w_4] | w_k \in \{0.1, 0.7\}\}$. Discount factor is 0.99. We used a NN with 1 hidden layer of 128 nodes for the DQN to train the DF policy. We used a NN with 1 hidden layer of 1024 nodes and 13 outputs to compute the Q-functions for all w ’s in RDF training. We used the same architecture to learn Q-functions for all training models (RDF, DF, MLE, DF-Oracle) during the deployment. We provide further details in the supplement.

Conclusions from HIV Treatment Simulator

RDF learns a higher return policy with fewer adverse effects when evaluated on deployment-phase rewards in comparison to DF and MLE Since the RDF objective optimizes model parameters to have high performance both during learning and deployment, it can manage the trade-off between viral load and immune response more effectively than DF and MLE. In doing so, RDF produces a policy with consistently higher returns (Fig 5, lower middle) and

fewer adverse effects in HIV treatment. Specifically, we see the RDF policy consistently produces an improved immune response in terms of both types of T-cells (T^1 and E) and can reduce the viral load within the first 200 days (see Fig 5, right). This policy consists of administering *both RTIs and PIs* within the first 200 days to prevent subsequent development of strains that would otherwise be resistant to either drug class alone (Fig 5, right). However, we can also down-weight the preference for a specific drug category, as seen for PIs in Fig 5 (left column of HIV trajectories).

RDF offers significant advantages, even when dealing with more complex trade-offs, i.e. higher dimensional w Unlike the synthetic domains and the Cancer domain, the reward for the HIV domain consists of four different objectives namely, minimizing the viral load, maximizing the cytotoxic T-cells, and minimizing the adverse effects of RTIs and PIs as described in Eqs 16 and 17. The performance advantages of RDF are sustained across higher dimensional w in comparison to DF and MLE.

RDF can be applied to a broad range of policy optimizers. Unlike the other domains where we used LQR and VI planners, for the HIV domain we use DQN to perform policy optimization. Regardless of this choice, RDF consistently outperforms DF and MLE.

Performing RDF in higher dimensions is computationally efficient. For the synthetic and Cancer domains, running LQR and VI optimization at each planning step is fast. However, in the HIV domain, with DQNs, one would typically need $|W|$ policies. Our results show we can use one network to *both amortize the cost of computing and store the Q-values* for RDF under multiple reward preferences.

8 DISCUSSION

In this paper, we introduced the Robust Decision-focused Model-based RL framework (RDF) as a novel approach for learning transition models in settings with varying reward preferences.

From a technical perspective, and important aspect was addressing the time and space complexity requirements of the RDF framework. We demonstrated that our RDF framework can use a number of different policy optimisers. Some settings were small enough such that we could apply Value Iteration to learn the optimal action-value function at each planning step. In other settings, such as the cancer simulator, we combined our RDF framework with a Linear Quadratic Regulator (LQR) planner to make that planning step more efficient. This is an example of situation in which using a restricted model class (linear) also created computational efficiencies for the robust optimization.

To scale to more reward bases and more complex environments, we integrated our RDF framework with DQNs as the planners. Learning an optimal action-value function at each planning step was no longer computationally feasible. To overcome this limitation, we leveraged past work which showed that interleaving Q- and model-updates is possible to achieve convergence for DF [23]. However, we discovered that unlike in previous approaches, higher quality inverse Jacobian estimates were required while computing the model gradients using implicit gradients—and adapted our optimization to do so. Understanding the conditions when a better approximation is required in DF-MBRL is an important avenue for future work. Further, we used a single network to amortize the cost of computing and storing Q-values for RDF learning with multiple rewards. These contributions mitigate the computational

burden associated with RDF, making it more practical for real-world applications.

Finally, we considered the setting where the policy is learned after the reward preference is observed at deployment time. Investigating the integration of MORL techniques with RDF framework to enhance the learn models and policies in a decision-focused manner is a promising direction for future work.

REFERENCES

- [1] Axel Abels, Diederik Roijers, Tom Lenaerts, Ann Nowé, and Denis Steckelmacher. 2019. Dynamic Weights in Multi-Objective Deep Reinforcement Learning. In *Proceedings of the 36th International Conference on Machine Learning*. PMLR, 11–20. <https://proceedings.mlr.press/v97/abels19a.html> ISSN: 2640-3498.
- [2] Brian Michael Adams, Harvey Thomas Banks, Hee-Dae Kwon, and Hien T Tran. 2004. *Dynamic multidrug therapies for HIV: Optimal and STI control approaches*. Technical Report. North Carolina State University. Center for Research in Scientific Computation.
- [3] Andre Barreto, Diana Borsa, John Quan, Tom Schaul, David Silver, Matteo Hessel, Daniel Mankowitz, Augustin Zidek, and Remi Munos. 2018. Transfer in deep reinforcement learning using successor features and generalised policy improvement. In *International Conference on Machine Learning*. PMLR, 501–510.
- [4] André Barreto, Shaobo Hou, Diana Borsa, David Silver, and Doina Precup. 2020. Fast reinforcement learning with generalized policy updates. *Proceedings of the National Academy of Sciences* 117, 48 (Dec 2020), 30079–30087. <https://doi.org/10.1073/pnas.1907370117>
- [5] Leon Barrett and Srin Narayanan. 2008. Learning All Optimal Policies with Multiple Criteria. In *Proceedings of the 25th International Conference on Machine Learning (ICML '08)*. Association for Computing Machinery, New York, NY, USA, 41–47. <https://doi.org/10.1145/1390156.1390162> event-place: Helsinki, Finland.
- [6] Marc Peter Deisenroth. 2011. A Survey on Policy Search for Robotics. *Foundations and Trends in Robotics* 2, 1–2 (2011), 1–142. <https://doi.org/10.1561/23000000021>
- [7] Esther Derman, Matthieu Geist, and Shie Mannor. 2021. Twice regularized MDPs and the equivalence between robustness and regularization. *Advances in Neural Information Processing Systems* 34 (2021), 22274–22287.
- [8] Finale Doshi-Velez and Been Kim. 2017. Towards a rigorous science of interpretable machine learning. *arXiv preprint arXiv:1702.08608* (2017).
- [9] Damien Ernst, Pierre Geurts, and Louis Wehenkel. 2005. Tree-based batch mode reinforcement learning. *Journal of Machine Learning Research* 6 (2005).
- [10] Damien Ernst, Guy-Bart Stan, Jorge Goncalves, and Louis Wehenkel. 2006. Clinical data based optimal STI strategies for HIV: a reinforcement learning approach. In *Proceedings of the 45th IEEE Conference on Decision and Control*. IEEE, 667–672.
- [11] Amir-massoud Farahmand. 2018. Iterative Value-Aware Model Learning. In *Advances in Neural Information Processing Systems*, Vol. 31. Curran Associates, Inc. <https://papers.nips.cc/paper/2018/hash/7a2347d96752880e3d58d72e9813cc14-Abstract.html>
- [12] Amir-Massoud Farahmand, Andre Barreto, and Daniel Nikovski. 2017. Value-Aware Loss Function for Model-based Reinforcement Learning. In *Proceedings of the 20th International Conference on Artificial Intelligence and Statistics*. PMLR, 1486–1494. <https://proceedings.mlr.press/v54/farahmand17a.html> ISSN: 2640-3498.
- [13] Joseph Futoma, Michael Hughes, and Finale Doshi-Velez. 2020. POPCORN: Partially Observed Prediction Constrained Reinforcement Learning. In *Proceedings of the Twenty Third International Conference on Artificial Intelligence and Statistics*. PMLR, 3578–3588. <https://proceedings.mlr.press/v108/futoma20a.html> ISSN: 2640-3498.
- [14] Christopher Grimm, Andre Barreto, Satinder Singh, and David Silver. 2020. The Value Equivalence Principle for Model-Based Reinforcement Learning. In *Advances in Neural Information Processing Systems*, H. Larochelle, M. Ranzato, R. Hadsell, M.F. Balcan, and H. Lin (Eds.), Vol. 33. Curran Associates, Inc., 5541–5552. https://proceedings.neurips.cc/paper_files/paper/2020/file/3bb585ea00014b0e3ebe4c6dd165a358-Paper.pdf
- [15] Bryan A. Hassell, Girija Goyal, Esak Lee, Alexandra Sontheimer-Phelps, Oren Levy, Christopher S. Chen, and Donald E. Ingber. 2017. Human Organ Chip Models Recapitulate Orthotopic Lung Cancer Growth, Therapeutic Responses, and Tumor Dormancy In Vitro. *Cell Reports* 21, 2 (Oct 2017), 508–516. <https://doi.org/10.1016/j.celrep.2017.09.043>
- [16] Conor F. Hayes, Roxana Rădulescu, Eugenio Bargiacchi, Johan Källström, Matthew Macfarlane, Mathieu Reymond, Timothy Verstraeten, Luisa M. Zintgraf, Richard Dazeley, Fredrik Heintz, Enda Howley, Athirai A. Irissappane, Patrick Mannion, Ann Nowé, Gabriel Ramos, Marcello Restelli, Peter Vamplew, and Diederik M. Roijers. 2022. A practical guide to multi-objective reinforcement learning and planning. *Autonomous Agents and Multi-Agent Systems* 36, 1 (April 2022), 26. <https://doi.org/10.1007/s10458-022-09552-y>
- [17] Hisham Husain, Kamil Ciosek, and Ryota Tomioka. 2021. Regularized Policies are Reward Robust. In *Proceedings of The 24th International Conference on Artificial Intelligence and Statistics*. PMLR, 64–72. <https://proceedings.mlr.press/v130/husain21a.html>
- [18] Donald E. Ingber. 2022. Human organs-on-chips for disease modelling, drug development and personalized medicine. *Nature Reviews Genetics* 23, 88 (Aug 2022), 467–491. <https://doi.org/10.1038/s41576-022-00466-9>
- [19] Joshua Joseph, Alborz Geramifard, John W. Roberts, Jonathan P. How, and Nicholas Roy. 2013. Reinforcement learning with misspecified model classes. In *2013 IEEE International Conference on Robotics and Automation*. 939–946. <https://doi.org/10.1109/ICRA.2013.6630686> ISSN: 1050-4729.
- [20] Daniel J. Lizotte, Michael Bowling, and Susan A. Murphy. 2010. Efficient Reinforcement Learning with Multiple Reward Functions for Randomized Controlled Trial Analysis. In *Proceedings of the 27th International Conference on International Conference on Machine Learning (ICML '10)*. Omnipress, Madison, WI, USA, 695–702. event-place: Haifa, Israel.
- [21] Volodymyr Mnih, Koray Kavukcuoglu, David Silver, Andrei A. Rusu, Joel Veness, Marc G. Bellemare, Alex Graves, Martin Riedmiller, Andreas K. Fidjeland, Georg Ostrovski, Stig Petersen, Charles Beattie, Amir Sadik, Ioannis Antonoglou, Helen King, Dharmashan Kumar, Dan Wierstra, Shane Legg, and Demis Hassabis. 2015. Human-level control through deep reinforcement learning. *Nature* 518, 75407540 (Feb 2015), 529–533. <https://doi.org/10.1038/nature14236>
- [22] Hossam Mossalam, Yannis M. Assael, Diederik M. Roijers, and Shimon Whiteson. 2016. Multi-Objective Deep Reinforcement Learning. <http://arxiv.org/abs/1610.02707> arXiv:1610.02707 [cs].
- [23] Evgenii Nikishin, Romina Abachi, Rishabh Agarwal, and Pierre-Luc Bacon. 2022. Control-Oriented Model-Based Reinforcement Learning with Implicit Differentiation. *Proceedings of the AAAI Conference on Artificial Intelligence* 36, 7 (June 2022), 7886–7894. <https://doi.org/10.1609/aaai.v36i7.20758> Number: 7.
- [24] Chris Reinke and Xavier Alameda-Pineda. 2021. Xi-learning: Successor feature transfer learning for general reward functions. *arXiv preprint arXiv:2110.15701* (2021).
- [25] Benjamin Ribba, Gentian Kaloshi, Mathieu Peyre, Damien Ricard, Vincent Calvez, Michel Tod, Branka Čajavec Bernard, Ahmed Idbaih, Dimitri Psimaras, Linda Dainese, Johan Pallud, Stéphanie Cartalat-Carel, Jean-Yves Delattre, Jérôme Honorat, Emmanuel Grenier, and François Ducray. 2012. A Tumor Growth Inhibition Model for Low-Grade Glioma Treated with Chemotherapy or Radiotherapy. *Clinical Cancer Research* 18, 18 (Sept. 2012), 5071–5080. <https://doi.org/10.1158/1078-0432.CCR-12-0084>
- [26] Tom Schaul, Georg Ostrovski, Iurii Kemaev, and Diana Borsa. 2021. Return-based scaling: Yet another normalisation trick for deep RL. *arXiv preprint arXiv:2105.05347* (2021).
- [27] Abhishek Sharma, Catherine Zeng, Sanjana Narayanan, Sonali Parbhoo, and Finale Doshi-Velez. 2021. On learning prediction-focused mixtures. *arXiv preprint arXiv:2110.13221* (2021).
- [28] Richard S. Sutton. 1991. Dyna, an integrated architecture for learning, planning, and reacting. *ACM SIGART Bulletin* 2, 4 (July 1991), 160–163. <https://doi.org/10.1145/122344.122377>
- [29] Richard S Sutton and Andrew G Barto. 2018. *Reinforcement learning: An introduction*. MIT press.
- [30] Peter Vamplew, Richard Dazeley, Adam Berry, Rustam Issabekov, and Evan Dekker. 2011. Empirical evaluation methods for multiobjective reinforcement learning algorithms. *Machine Learning* 84, 1-2 (July 2011), 51–80. <https://doi.org/10.1007/s10994-010-5232-5>
- [31] Runzhe Wan, Xinyu Zhang, and Rui Song. 2021. Multi-Objective Model-based Reinforcement Learning for Infectious Disease Control (*KDD '21*). Association for Computing Machinery, New York, NY, USA, 1634–1644. <https://doi.org/10.1145/3447548.3467303>
- [32] Kai Wang, Sanket Shah, Haipeng Chen, Andrew Perrault, Finale Doshi-Velez, and Milind Tambe. 2021. Learning MDPs from Features: Predict-Then-Optimize for Sequential Decision Making by Reinforcement Learning. In *Advances in Neural Information Processing Systems*, Vol. 34. Curran Associates, Inc., 8795–8806. <https://proceedings.neurips.cc/paper/2021/hash/49e863b146f3b5470ee222ee84669b1c-Abstract.html>
- [33] Marco A. Wiering, Maikel Withagen, and Mădălina M Drugan. 2014. Model-based multi-objective reinforcement learning. In *2014 IEEE Symposium on Adaptive Dynamic Programming and Reinforcement Learning (ADPRL)*. 1–6. <https://doi.org/10.1109/ADPRL.2014.7010622> ISSN: 2325-1867.
- [34] Bryan Wilder, Eric Ewing, Bistra Dilkina, and Milind Tambe. 2019. End to end learning and optimization on graphs. In *Advances in Neural Information Processing Systems*, Vol. 32. Curran Associates, Inc. <https://proceedings.neurips.cc/paper/2019/hash/8bd39eac38511daad6152e84545e504d-Abstract.html>
- [35] Tomohiro Yamaguchi, Shota Nagahama, Yoshihiro Ichikawa, and Keiki Takadama. 2019. Model-Based Multi-objective Reinforcement Learning with Unknown Weights. In *Human Interface and the Management of Information. Information in Intelligent Systems (Lecture Notes in Computer Science)*, Sakae Yamamoto and Hirohiko Mori (Eds.). Springer International Publishing, Cham, 311–321. https://doi.org/10.1007/978-3-030-22649-7_25
- [36] Gregory Yauney and Pratik Shah. 2018. Reinforcement Learning with Action-Derived Rewards for Chemotherapy and Clinical Trial Dosing Regimen Selection.

In *Proceedings of the 3rd Machine Learning for Healthcare Conference*. PMLR, 161–226. <https://proceedings.mlr.press/v85/yauney18a.html> ISSN: 2640-3498.

A ALTERNATE RDF OBJECTIVE FORMULATION

The RDF objective can also be formulated in the integral terms

$$\begin{aligned} \theta_{\text{RDF}} \leftarrow \arg \min_{\theta} \int_{w \in \mathcal{U}} L_{T^*, R_w}(\theta) dw \\ \text{s.t. } J_{T^*, R_{\bar{w}}}(\pi^*(\theta, R_{\bar{w}})) \geq \delta \end{aligned} \quad (18)$$

where \mathcal{U} specifies the region over which we wish to be robust over.

While this objective is equivalent to the objective in Eqn 8 under the assumption that $P(w)$ is a uniform measure on the domain of \mathcal{U} , it has an intuitive interpretation: we wish to maximize the volume of the return achieved by our model θ . This intuition also motivates why we choose a uniform measure for $P(w)$.

CHOOSING A POLICY PLANNER FOR RDF

Choosing a specific simple model class enables fast planning, e.g. value iteration for discrete states and Linear Quadratic Regulator (LQR) for continuous states with linear dynamics.

When using a DQN to represent the Q-function, we used the same network to compute the Q-values for each w , which allowed us to amortize the cost of learning the Q-function across different w 's. Such an approach has been demonstrated to be effective in a multi-task and multi-objective reinforcement learning setting [1, 3]. However, scaling the losses (as per [26]) to account for the relative difference in reward ranges was crucial for stability. If \mathcal{W} (in Eq 13) can change, e.g. when using an adaptive method to approximate Eq 12, such an architecture just requires us to just add a sub-network if a new w is added, and replace an existing sub-network if an existing w is replaced.

B PROOF FOR THEOREM 1

THEOREM B.1. *Let $R_{\bar{w}}$ be the learning-phase reward function with preference \bar{w} , and R_w be the reward function with an arbitrary preference w . Let Q_w^* be the optimal action-value function for the true MDP for reward function R_w . Let $B_w, \hat{B}_w^{DF}, \hat{B}_w^{RDF}$ denote the Bellman optimality operators under the true dynamics, DF model and RDF model respectively.*

Assume \hat{Q}_w^{DF} and \hat{Q}_w^{RDF} are fixed points under \hat{B}_w^{DF} and \hat{B}_w^{RDF} respectively. Further assume that the reward function is bounded, $R_w(s, a) \in [0, r_{\max}] \forall s, a, w$.

DF Case. Consider a DF model trained on $R_{\bar{w}}$. If the Bellman operator induced by the DF model achieves the error

$$\sup_{s,a} |B_{\bar{w}} \hat{Q}_{\bar{w}}^{DF}(s, a) - \hat{B}_{\bar{w}}^{DF} \hat{Q}_{\bar{w}}^{DF}(s, a)| = \epsilon_{\bar{w}}^{DF},$$

then

$$Q_w^*(s, a) - \hat{Q}_w^{DF}(s, a) \leq \frac{\epsilon_w^{DF}}{(1-\gamma)} \quad \text{for } w = \bar{w} \quad (19)$$

$$Q_w^*(s, a) - \hat{Q}_w^{DF}(s, a) \leq \gamma \frac{r_{\max}}{(1-\gamma)^2} \quad \forall w \neq \bar{w} \quad (20)$$

RDF Case. Consider the RDF model trained with learning-phase preference \bar{w} and deployment-phase reward preference distribution $P(w)$. For a $w \in P(w)$, if the Bellman operator \hat{B}_w^{RDF} induced by the RDF model achieves the error

$$\sup_{s,a} |B_w \hat{Q}_w^{RDF}(s, a) - \hat{B}_w^{RDF} \hat{Q}_w^{RDF}(s, a)| = \epsilon_w^{RDF},$$

then

$$Q_w^*(s, a) - \hat{Q}_w^{RDF}(s, a) \leq \frac{\epsilon_w^{RDF}}{(1-\gamma)} \quad (21)$$

For, $w \neq \bar{w}$, the RDF bound is tighter since we explicitly optimize ϵ_w^{RDF} whereas $\gamma \frac{r_{\max}}{(1-\gamma)^2}$ is constant.

PROOF. First, we show the bound for the RDF and DF($w = \bar{w}$) case. Then we show the DF($w \neq \bar{w}$) bound.

RDF and DF($w = \bar{w}$) case. $\forall s, a$ our Q approximation can be written as follows,

$$\left| Q_w^*(s, a) - \hat{Q}_w^{RDF}(s, a) \right| \quad (22)$$

$$= \left| B_w Q_w^*(s, a) - \hat{B}_w^{RDF} \hat{Q}_w^{RDF}(s, a) \right| \quad (23)$$

$$\leq \left| B_w \hat{Q}_w^{RDF}(s, a) - \hat{B}_w^{RDF} \hat{Q}_w^{RDF}(s, a) \right| + \left| B_w Q_w^*(s, a) - B_w \hat{Q}_w^{RDF}(s, a) \right| \quad (24)$$

$$= \epsilon_w^{RDF} + \left| r_w(s, a) + \gamma \mathbb{E}_{T^*(s, a)} \left[\max_{a'} Q_w^*(s', a') \right] - r_w(s, a) - \gamma \mathbb{E}_{T^*(s, a)} \left[\max_{a'} \hat{Q}_w^{RDF}(s', a') \right] \right| \quad (25)$$

$$= \epsilon_w^{RDF} + \gamma \left| \mathbb{E}_{T^*(s, a)} \left[\max_{a'} Q_w^*(s', a') - \max_{a'} \hat{Q}_w^{RDF}(s', a') \right] \right| \quad (26)$$

$$\leq \epsilon_w^{RDF} + \gamma \|T^*(s, a)\|_1 \left\| \max_{a'} Q_w^*(\cdot, a') - \max_{a'} \hat{Q}_w^{RDF}(\cdot, a') \right\|_\infty \quad (27)$$

$$\leq \epsilon_w^{RDF} + \gamma \max_{s', a'} \left| Q_w^*(s', a') - \hat{Q}_w^{RDF}(s', a') \right| \quad (28)$$

Taking a max over s, a yields

$$\max_{s, a} \left| Q_w^*(s, a) - \hat{Q}_w^{RDF}(s, a) \right| \leq \epsilon_w^{RDF} + \gamma \max_{s, a} \left| Q_w^*(s, a) - \hat{Q}_w^{RDF}(s, a) \right| \quad (29)$$

$$\implies \max_{s, a} \left| Q_w^*(s, a) - \hat{Q}_w^{RDF}(s, a) \right| \leq \frac{\epsilon_w^{RDF}}{(1 - \gamma)} \quad (30)$$

For the DF($w = \bar{w}$) case, we get an analogous bound:

$$\max_{s, a} \left| Q_{\bar{w}}^*(s, a) - \hat{Q}_{\bar{w}}^{DF}(s, a) \right| \leq \frac{\epsilon_{\bar{w}}^{DF}}{(1 - \gamma)} \quad (31)$$

DF($w \neq \bar{w}$) case. First, we show that for any $Q(s, a)$ and $w \neq \bar{w}$,

$$\left| B_w Q(s, a) - \hat{B}_w^{DF} Q(s, a) \right| \quad (32)$$

$$= \gamma \left| \mathbb{E}_{T^*(s, a) - T^{DF}(s, a)} \left[\max_{a'} Q(s', a') \right] \right| \quad (33)$$

$$\leq \gamma \left| \mathbb{E}_{T^*(s, a) - T^{DF}(s, a)} \left[\max_{a'} Q(s', a') \right] - \frac{r_{max}}{2(1 - \gamma)} \right| \quad (34)$$

$$\leq \gamma \|T^*(s, a) - T^{DF}(s, a)\|_1 \left\| \max_{a'} Q(\cdot, a') - \frac{r_{max}}{2(1 - \gamma)} \mathbf{1} \right\|_\infty \quad (35)$$

$$\leq \gamma \|T^*(s, a) - T^{DF}(s, a)\|_1 \frac{r_{max}}{2(1 - \gamma)} \quad (36)$$

$$\leq \gamma \frac{r_{max}}{(1 - \gamma)} \quad (37)$$

Now, for a (s, a) and $w \neq \bar{w}$

$$\left| Q_w^*(s, a) - \hat{Q}_w^{DF}(s, a) \right| \quad (38)$$

$$= \left| B_w Q_w^*(s, a) - \hat{B}_w^{DF} \hat{Q}_w^{DF}(s, a) \right| \quad (39)$$

$$\leq \left| B_w \hat{Q}_w^{DF}(s, a) - \hat{B}_w^{DF} \hat{Q}_w^{DF}(s, a) \right| + \left| B_w Q_w^*(s, a) - B_w \hat{Q}_w^{DF}(s, a) \right| \quad (40)$$

$$\leq \left| B_w \hat{Q}_w^{DF}(s, a) - \hat{B}_w^{DF} \hat{Q}_w^{DF}(s, a) \right| + \gamma \max_{s', a'} \left| Q_w^*(s', a') - \hat{Q}_w^{DF}(s', a') \right| \quad (41)$$

$$\leq \gamma \frac{r_{max}}{(1 - \gamma)} + \gamma \max_{s', a'} \left| Q_w^*(s', a') - \hat{Q}_w^{DF}(s', a') \right| \quad (42)$$

which yields

$$\max_{s, a} \left| Q_w^*(s, a) - \hat{Q}_w^{DF}(s, a) \right| \leq \gamma \frac{r_{max}}{(1 - \gamma)^2} \quad (43)$$

□

C EXPERIMENTAL DETAILS

C.1 Synthetic MDP

The transition matrix values were sampled from a standard normal distribution before being normalized using a softmax transformation. There are two reward matrices, and their values were uniformly sampled in $[-60, 40]$ before being clipped to $[0, 40]$.

We share the code for generating the synthetic MDP for validating the Theorem 1 in the main paper. The code is written in Python and uses PyTorch.

```
1 data_seed = 0
2 torch.manual_seed(data_seed)
3 num_actions, num_states = 2, 20
4 dtype_float = torch.float64
5
6 # Transition matrix
7 # Shape: [num_actions, num_states, num_states]
8 true_transition = torch.randn(num_actions, num_states, num_states, dtype=dtype_float)
9 true_transition = torch.softmax(true_transition, dim=-1)
10 true_transition[:, -1] = 0
11 true_transition[:, -1, -1] = 1
12
13 # Reward matrix
14 # Shape: [num_states, num_actions]
15 true_reward_1 = (torch.rand(num_states, num_actions, dtype=dtype_float))
16 true_reward_2 = (torch.rand(num_states, num_actions, dtype=dtype_float))
17 true_reward_1 = true_reward_1.clamp(0.6,) - 0.6
18 true_reward_2 = true_reward_2.clamp(0.6,) - 0.6
19 true_reward_1 *= 100
20 true_reward_2 *= 100
21 true_reward_1[-1, :] = 0
22 true_reward_2[-1, :] = 0
23 get_true_reward = lambda w: true_reward_1 * w + true_reward_2 * (1 - w)
24
25 gamma = 0.9
26 temperature = 0.01
```

MOUNTAINCAR ENVIRONMENT

In this environment, an underpowered car is positioned in a valley between two mountains on a one-dimensional track. The aim is to drive the car to the mountain top on the right-hand side, but the engine power available is insufficient to accelerate and power through to the top. The agent must build momentum by moving between the two mountains until the car has sufficient momentum to reach its goal. The states are in \mathbb{R}^2 and correspond to the current position and velocity. The actions are in $\{-1, 0, 1\}$ and correspond to accelerating backward, not accelerating, and accelerating forwards respectively. An episode runs for a maximum of 200 steps.

Transition model learning. While the true dynamics follow the equations of motion, we learn a tabular representation of the transition dynamics by discretizing the state space, which frequently used in RL [29]. We split the position and velocity to 15 bins each, resulting in a total of 225 states. We can then use Value Iteration to derive the optimal policy at each step of the optimization.

We set the learning-phase reward preference to $\bar{w} = 0.95$, and the deployment-phase reward preferences range to $w \in [0.75, 1]$. The discount factor is 1. We backpropagate through the fixed point of the Bellman operator to compute the gradients with respect to tabular model values (Eq (14)).

Reward function. The first reward basis function R_1 is a penalty of -1 for each time step, whereas the second reward basis function R_2 is a penalty of -0.1 each time the car accelerates as a proxy for fuel consumption.

$$R_1(s) = -1; \quad R_2(a) = \begin{cases} 0, & \text{if } a = 0 \\ -0.1, & \text{o/w.} \end{cases}$$

In the single-objective problem focusing solely on R_1 , the agent only needs to reach the goal in fewest number of steps. By including R_2 , we force the agent to exhibit prudence in its use of acceleration.

HIV TREATMENT

We set the $\bar{w} = [0.25, 0.25, 0.25, 0.25]$. The deployment preference weights range (w) was set to the simplex formed by spanning points $\{[w_1, w_2, w_3, w_4] | w_k \in \{0.1, 0.7\}\}$. To efficiently sample a range of points, we employed a "triangulation" technique, selecting 13 points for the experiment. The value in $\mathcal{W} \cup \{\bar{w}\}$ were:

0.25	0.25	0.25	0.25
0.1	0.1	0.1	0.7
0.1	0.1	0.7	0.1
0.1	0.3	0.3	0.3
0.1	0.7	0.1	0.1
0.2	0.2	0.2	0.4
0.2	0.2	0.4	0.2
0.2	0.4	0.2	0.2
0.3	0.1	0.3	0.3
0.3	0.3	0.1	0.3
0.3	0.3	0.3	0.1
0.4	0.2	0.2	0.2
0.7	0.1	0.1	0.1

We used a neural net with 1 hidden layer of 128 nodes for the DQN to train the DF policy. We used a neural net with 1 hidden layer of 1024 nodes and 13 outputs to compute the Q-functions for all w 's in RDF training. We used the same architecture to learn Q-functions for all training models (RDF, DF, MLE, DF-Oracle) during the deployment.

We computed gradients for the transition model parameters θ using Eq 14. We note that computing a reasonable estimate of the inverse Jacobian term was necessary for DF and RDF methods to work in our experiments, contrary to past work where inverse Jacobian was approximated by an identity matrix [23, 32]. We conjecture that this is due to the complexity of the HIV domain. We ran the Conjugate Gradient method for 10 iterations to approximate the inverse Jacobian.

D ADDITIONAL PLOTS

D.1 Cancer Treatment

D.1.1 Sensitivity analysis for λ and δ parameters. The optimization problem in Eqn 8 is solved by the saddle-point algorithm, where the Lagrange multiplier λ is updated depending on whether the constraint is satisfied or not. However, we can also solve the optimization problem by fixing λ and running the optimization on a grid of such λ values.

Below, we show the implicit constraint value δ achieved by the optimization problem for different values of λ .

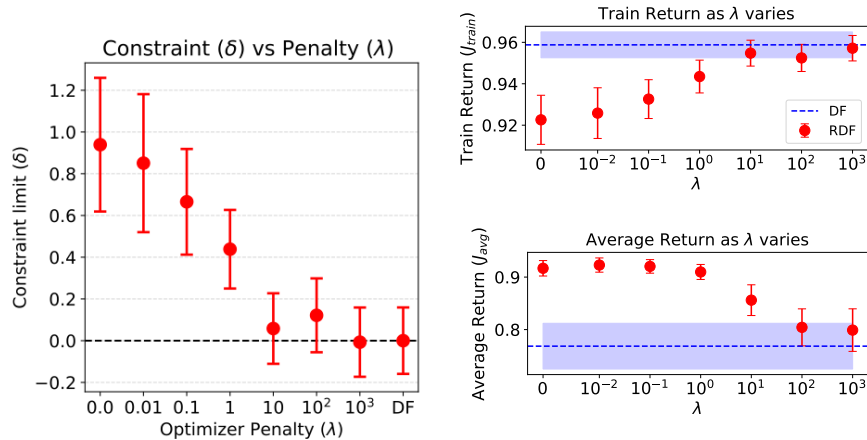


Figure 6: Sensitivity analysis of the λ hyperparameter.

Mean Tumor Diameter Trajectories for different reward preferences - RDF

RDF ($\delta = 0.92$): Total Mean Tumor Diameters (MTD) Trajectories (Learning-phase preference, $\bar{w} = 0.75$)

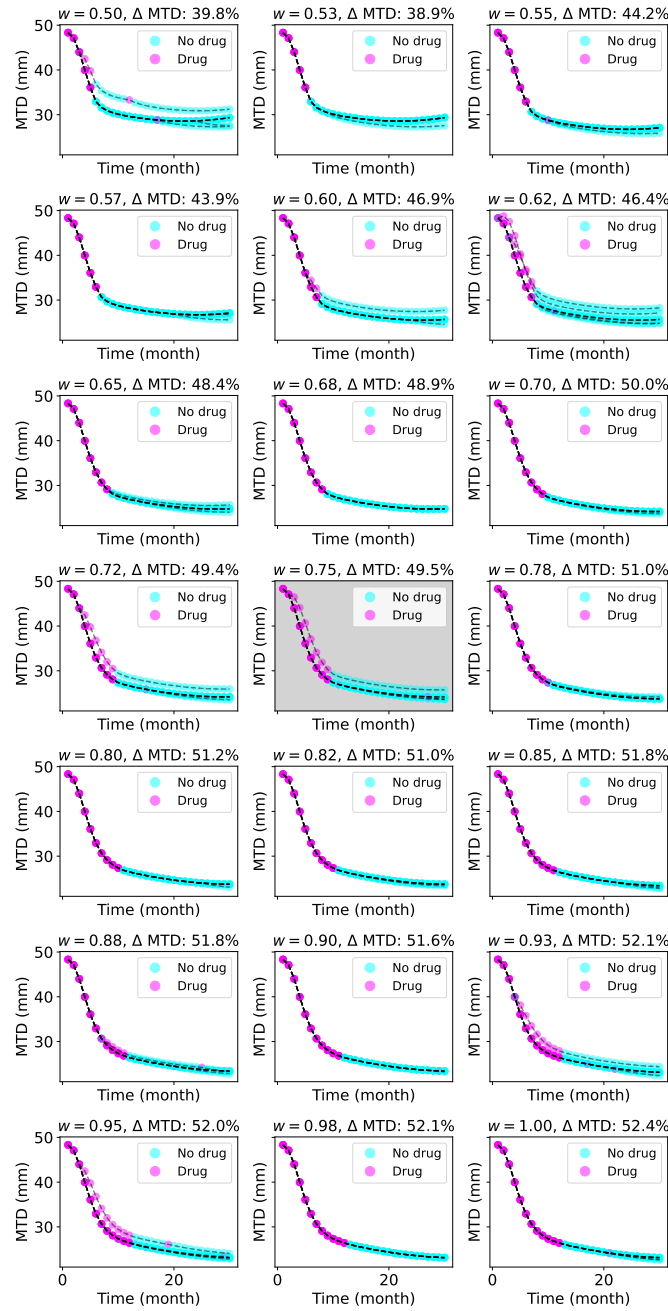


Figure 7: Mean tumor diameter trajectories for different reward preferences with the RDF model. The learning-phase reward preference is $\bar{w} = 0.75$ and the deployment-phase reward preference is $w \in [0.5, 1.0]$.

Mean Tumor Diameter Trajectories for different reward preferences - DF

DF: Total Mean Tumor Diameters (MTD) Trajectories (Learning-phase preference, $\bar{w} = 0.75$)

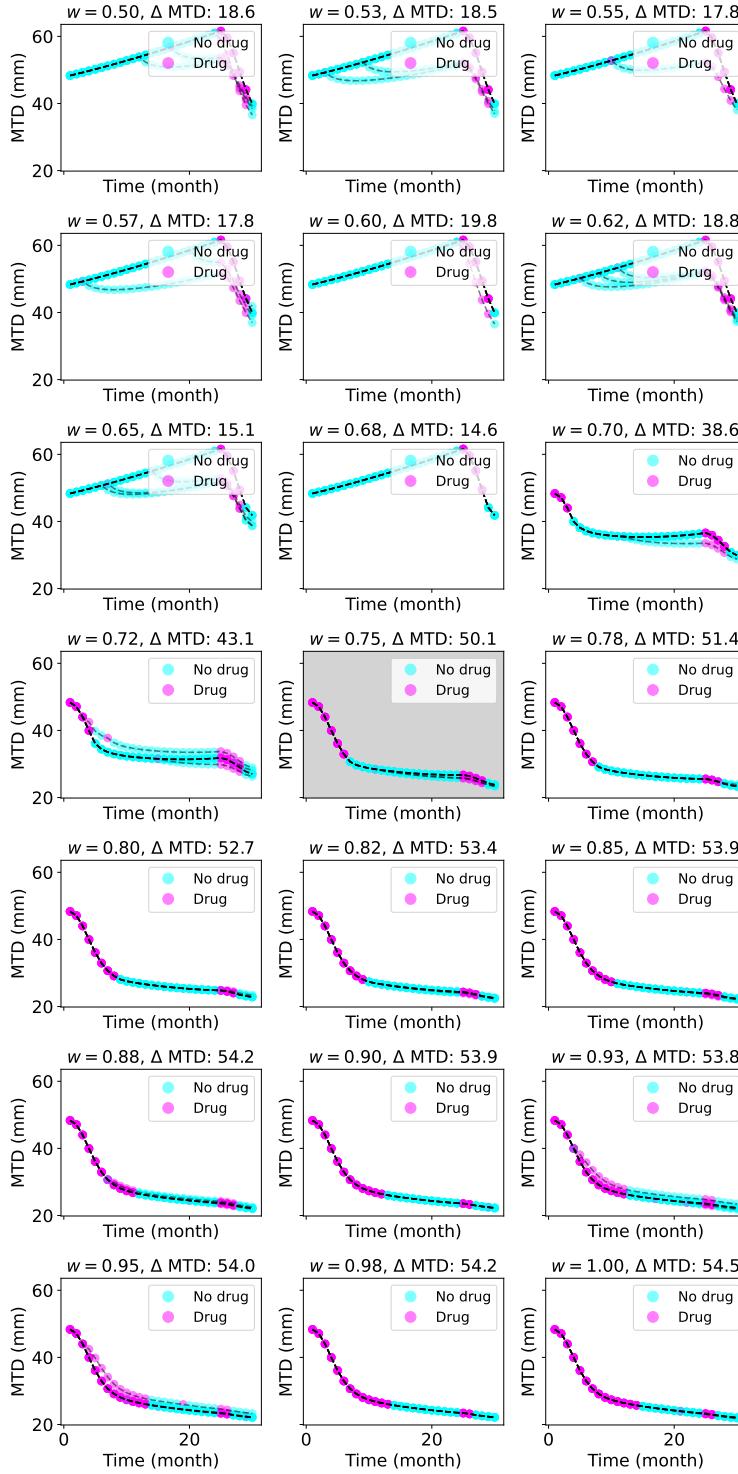


Figure 8: Mean tumor diameter trajectories for different reward preferences with the DF model. The learning-phase reward preference is $\bar{w} = 0.75$ and the deployment-phase reward preference is $w \in [0.5, 1.0]$.

Drug Concentration Trajectories for different reward preferences - RDF

RDF ($\delta = 0.92$): Drug Concentration Trajectories (Learning-phase preference, $\bar{w} = 0.75$)

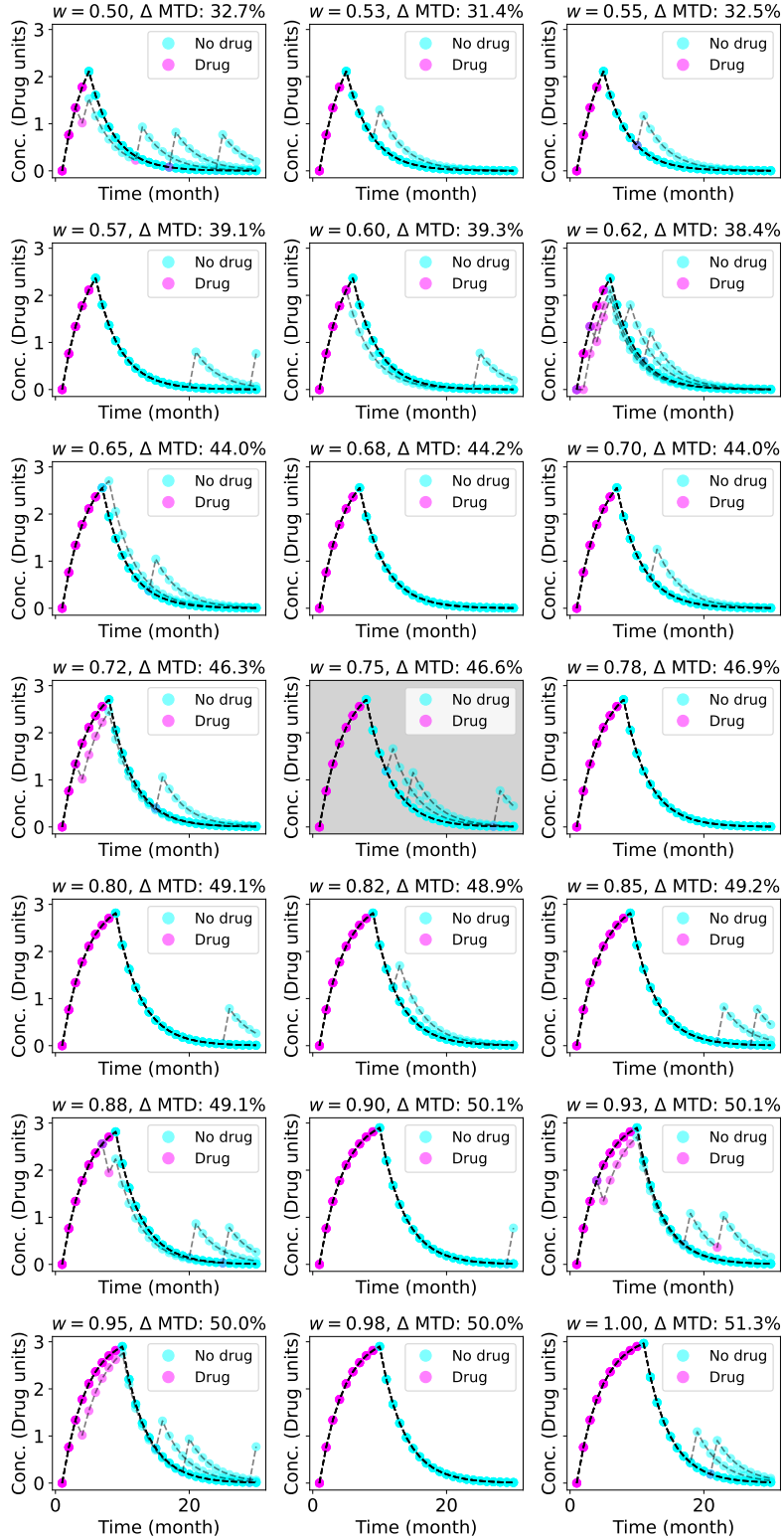


Figure 9: Mean tumor diameter trajectories for different reward preferences with the RDF model. The learning-phase reward preference is $\bar{w} = 0.75$ and the deployment-phase reward preference is $w \in [0.5, 1.0]$.

Drug Concentration Trajectories for different reward preferences - DF

DF: Drug Concentration Trajectories (Learning-phase preference, $\bar{w} = 0.75$)

